Materials Science-Poland, *Vol. 28*, *No. 3*, *2010*

Synthesis and properties of magnetic nanoparticles coated with biocompatible compounds

M. RĂCUCIU[1*], D.E. CREANGĂ[2], A. AIRINEI[3], D. CHICEA[1], V. BĂDESCU[4]

[1]Lucian Blaga University, Faculty of Science, Dr.Ratiu Street, No. 5–7, Sibiu, 550024, Romania

[2]Al. I. Cuza University, Faculty of Physics, 11A Blvd. Copou, 700506, Iasi, Romania

[3]P. Poni Institute of Macromolecular Chemistry Iasi, Romania

[4] National Institute of R&D for Technical Physics, 47 Blvd. D. Mangeron, Iasi, Romania

Syntheses and characterization of two types of systems of magnetic nanoparticles functionalized with biocompatible molecules have been presented. Two colloidal suspensions of iron oxide nanoparticles fabricated by the same co-precipitation method were obtained; the nanoparticles with perchloric acid ($HClO_4$) and with citric acid ($C_6H_8O_7$), were coated and dispersed in water. The structure at nanometric level of functionalized magnetic nanoparticles was analyzed, using data obtained from magnetic, rheological and structural measurements. Magnetic properties were discussed based on magnetization measurements. Fourier transform infrared absorption spectra have been recorded to obtain additional information on the composition of functionalized magnetic nanoparticles. To assess the optical properties of highly diluted suspensions, UV-VIS absorbance spectra were recorded. Light scattering anisotropy on functionalized magnetic nanoparticles was investigated as well. The dimensional distribution of the nanoparticles physical diameter was comparatively presented using the box-plot statistical method applied to the data provided by transmission electron microscopy.

Keywords: *magnetic nanoparticles; magnetic properties; TEM analysis; FTIR spectra; UV–VIS absorbance; light scattering anisotropy*

1. Introduction

Colloidal suspensions of magnetic particles have been studied since the early 1900s but interest of scientists increased in the 1960s with the production of stable concentrated suspensions of magnetic nanoparticles [1, 2]. Systems of magnetic nanoparticles led to a significant number of commercial applications [3, 4]. Recent development of a large variety of functionalized magnetic nanoparticles resulted in

*Corresponding author, e-mail: mracuciu@yahoo.com

new biomedical and clinic applications. A major drawback for a lot of applications remains the lack of well-defined and characterized nanoparticles. Growing attention is paid to iron oxide nanoparticles (especially magnetite – Fe_3O_4) embedded in a biocompatible compound. Magnetic fluids consist of colloidal suspensions of ferromagnetic monodomain nanosized particles in various carrier liquids [3]. To avoid agglomeration of magnetic nanoparticles due to attractive van der Waals forces, the particles need to be coated with different complex agents that provide enhanced stability due to steric hidrance or combined electrostatic and steric stabilization. Synthetic and natural polyacids (e.g., dimercaptosuccinic acid, citric acid, tartaric acid, aspartic acid, glutamic acid) are the mostly used coating agents [5–7]. Among various methods for producing magnetic nanoparticles, chemical routes have the advantages of being relatively simple and providing good control over properties of the particles. Water based magnetic fluids hold great potential for biological applications, considering their influence in plant growth [8–11].

2. Experimental

Systems of magnetic nanoparticles were fabricated by alkaline hydrolysis of highly concentrated solutions of Fe^{2+} and Fe^{3+} salts following the preparation protocol proposed in [12]. Solutions of ferric and ferrous salts were prepared in 2 M HCl solvent since the acidic conditions prevent formation of iron hydroxides. 5.0 cm^3 of 2 M stock $FeCl_2$ solution and 20.0 cm^3 of 1 M stock $FeCl_3$ solution were added during magnetic mixing under continuous pouring of 250 cm^3 of 1 M NH_4OH solution.

The suspensions were finally washed with deionized water to reach approximately pH of 6.5. After washing, to the magnetic particles precipitate 5 cm^3 of 25% solution of perchloric acid (PA sample) or citric acid (CA sample) were added, the resulted dark suspension being further stirred for 1 h. The microstructural features of the two aqueous suspensions of the magnetic nanoparticles were analyzed by means of physical tests. The rheological properties such as density, dynamic viscosity and surface tension were measured using standard methods.

To obtain the profile of the nanoparticle dimensions, the magnetic measurements and transmission electron microscopy were chosen as main investigation methods. Using a Tesla device with the resolution of 1.0 nm, the transmission electron microscopy (TEM) images were obtained for 10^4 dilutions in distilled water of the samples, followed by the deposition on collodion sheet. Magnetization and magnetic susceptibility measurements were performed following the Gouy method at constant normal ambient temperature. Magnetic field intensity was measured by means Walker Scientific MG 50D Gaussmeter with a Hall probe and for sample weighting measurement an electronic balance ACULAB-200 with 10^{-4}g accuracy was used.

Infrared absorption spectra (FT-IR) have been recorded aiming to get some information upon the coated magnetic nanoparticles composition, using a Bruker Vertex 70

infrared spectrometer and magnetic nanoparticles dispersions in KBr after previous thermal treatment at 100 °C up to constant weight. To assess the optical properties of the highly diluted suspensions of magnetic nanoparticles, UV-VIS absorbance spectra were recorded with a CINTRA 5 spectrophotometer in a double beam mode, using a 1 cm quartz cell filled against deionized water as a reference solvent.

A typical light scattering procedure, with collimated laser beams was used to detec the far field [13–15], in assessing the light scattering properties of nanoparticles forming magnetic suspensions. A simple experimental setup was assembled, consisting of a He–Ne laser, a cuvette, a sensitive detector, a data acquisition system and a computer. The cuvette-detector distance D was 2.5 m and x was modified gradually, changing the angle accordingly. The detector was a photoresistor and had the dimension d of 5 mm which makes an angular opening of 0.002 rad or 0.1273°. For light scattering anisotropy studies, the initial magnetic nanoparticles suspensions were diluted at the volume ratio of 3.0×10^{-6}, using deionized water right before the light scattering analysis, in order to reduce the magnetic nanoparticles agglomeration rate that actually begins during dilution.

The light intensity that can be measured using a detector is proportional with the integral F of the phase function over the polar angle interval $[\theta_1, \theta_2]$ covered by the detector. The function F was fit on the experimental data using a program written for this purpose. Details of the experimental procedure are presented in [16].

3. Results and discussions

TEM images of PA and CA samples are shown in Fig. 1. The analyses of all TEM measurements resulted in physical diameter distribution histograms (Fig. 2), the mean of particles diameter being given in Table 1.

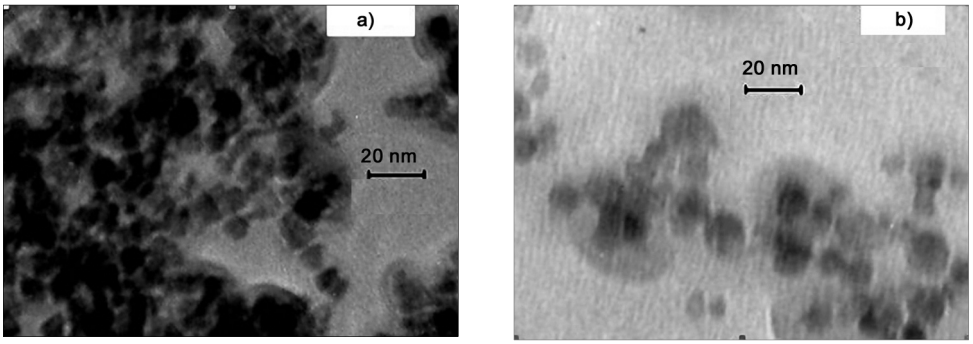

Fig. 1. TEM images of two systems of the functionalized magnetic nanoparticles analyzed in this study: a) CA sample, b) PA sample

Magnetization curves obtained for the functionalized magnetic nanoparticles samples are presented in Fig. 3. Considering the Langevin equation at high field and ex-

trapolating to $1/H = 0$, the magnetization (M) versus $1/H$ curves, the saturation magnetization was obtained. Also, the initial susceptibility χ_0 was determined from the slope of the magnetization versus magnetic filed curves at low field. Using magnetization measurements data and assuming a spherical particle shape, the magnetic diameters (d_M) were calculated according to Langevin's equation. The results are presented in Table 1.

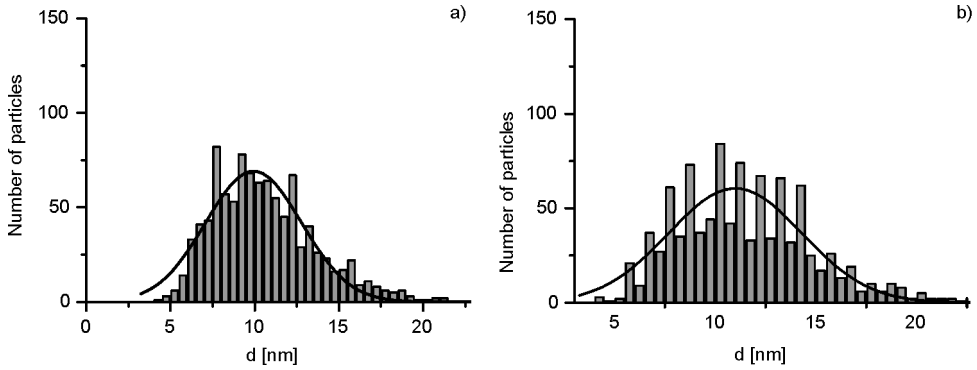

Fig. 2. Histogram of distributions of diameters of functionalized nanoparticles: a) PA, b) CA

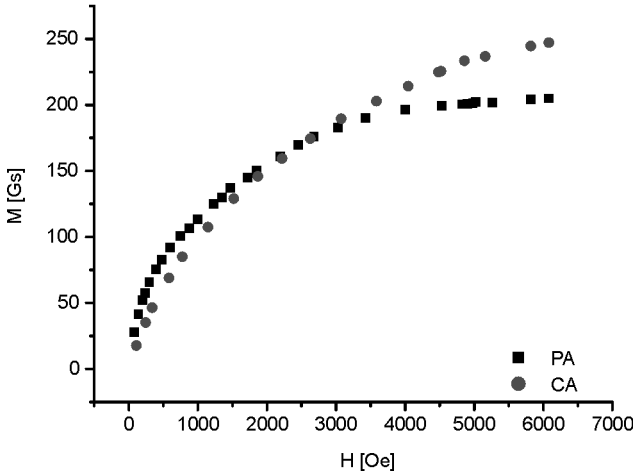

Fig. 3. Magnetization curves of the functionalized magnetic nanoparticles in aqueous suspensions

Table 1. The data for dimensional analysis and magnetic properties

Sample	ΦM [%]	d_{TEM} [nm]	d_M [nm]	M_S [Gs]	χ_0
PA	3.82	10.552	7.112	229.5	0.170
CA	4.67	11.448	6.014	280.5	0.107

Differences evidenced between d_{TEM} and d_M values can be assigned to the surfactant shell of the magnetite core. For these two types of coated magnetic nanoparticles, the thicknesses of the organic surface layers of 1.72 nm in the PA sample and of 2.71 nm in the CA sample have been calculated. Also, we can see that high magnetization value was revealed for the aqueous suspension of magnetic nanoparticles coated with citric acid. The results of measurements of the physical parameters as well as the volume fraction Φ, determined from the density measurements, are presented in Table 2.

Table 2. Rheological properties and volume fraction data

Sample	Φ [%]	Density [kg/m^3]	Surface tension $\times 10^3$ [N/m]	Viscosity $\times 10^3$ kg/(m·s)
PA	4.56	1088	86.7	1.8
CA	5.05	1089	77.1	2.7

Further analysis was carried out based on FTIR spectra (4000 cm^{-1}–500 cm^{-1}). In the magnetic nanoparticles coated with perchloric acid (PA sample) the FTIR spectra show a triple band at 1087 cm^{-1}, 1111 cm^{-1}, 1147 cm^{-1}and a double band at, 626 cm^{-1} and 637 cm^{-1} which confirms the presence of iron perchlorate in the solid phase of the PA coated magnetic nanoparticles system. The narrow but intense absorption of perchlorate ions at about 630 cm^{-1} seems to be overlapped onto weaker vibrations of the iron oxide skeleton situated in the same region.

Also, the 1400 cm^{-1} band could be assigned to the ferrophase complex vibrations. An intense band at 1610 cm^{-1} may be assigned to the deformation vibrations of water molecules trapped onto the magnetite colloidal particles. The low intensity and bifurcated bands at 3599 cm^{-1} and 3435cm^{-1} corresponding to OH symmetrical and asymmetrical stretchings can reveal the presence of free water traces. An intense absorption region beyond 600 cm^{-1} associated with stretching and torsional vibration modes of magnetite can also be seen.

In the CA sample, IR spectrum revealed the bands of iron citrate. An intense band at 3450 cm^{-1} confirms the presence of water traces while the absorption at 3200–3400 cm^{-1} suggests the presence of non-dissociated OH groups of citric acid. At 1600 cm^{-1}, an intense band is visible that may be assigned to the symmetric stretching of OH from COOH group, revealing the binding of a citric acid radical to the magnetite surface. Also, the neighbour band at 1400 cm^{-1} can be assigned to the asymmetric stretching of CO from COOH group. Low-intensity bands between 400 cm^{-1} and 600 cm^{-1} can be associated with stretching and torsional vibration modes of magnetite. Thus, we can say that the citric acid binds chemically to the magnetite surface by carboxylate chemisorptions, citrate ions resulting this way.

To assess the optical properties of highly diluted magnetite nanoparticles suspension (10^{-3} volume fraction), UV-VIS absorbance spectra were recorded on spectrophotometer in a double beam mode, with deionized water as reference solvent (Fig. 4).

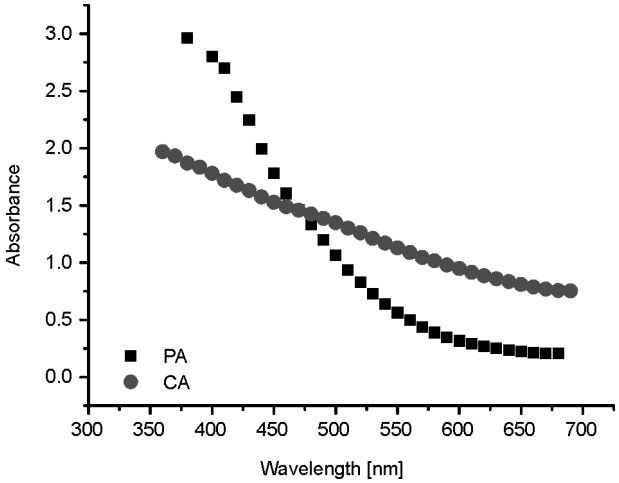

Fig. 4. UV-VIS absorbance spectra of the diluted suspensions of systems of magnetic nanoparticles

The PA sample exhibits an increased absorbance toward shorter wavelengths in comparison to the CA sample, while for longer wavelengths the CA sample exhibits an increased absorbance in comparison to PA sample.

For light scattering anisotropy study, two types of diluted magnetic nanoparticles suspensions (PA and CA) having the volume ratio of 3.0×10^{-6}, hence an optical depth around 1, to avoid multiple scattering, were used. For each sample, the light intensity was measured at various polar angles. The results of the fit that is the C and g values, the anisotropy parameter together with the errors in determining them with respect to the fit are presented in Table 3.

Table 3. The results of the light scattering anisotropy measurement on the magnetic nanoparticles systems analyzed in this study

Sample	Mean size [nm]	C [a.u.]	ΔC [a.u.]	g	Δg
PA	10.552	233.61	0.03	0.99108	10^{-5}
CA	11.448	304.23	0.01	0.98219	5×10^{-6}

Figure 5 presents the plot of the experimental data and of the F function calculated with the C and g values from the fit for CA sample. The light scattering anisotropy parameter was measured for both magnetic nanoparticles suspensions analyzed in this

study. Examining the data in Table 3,I we notice that the anisotropy parameter *g* of PA sample (0.99108) is higher than that for CA sample (0.98219).

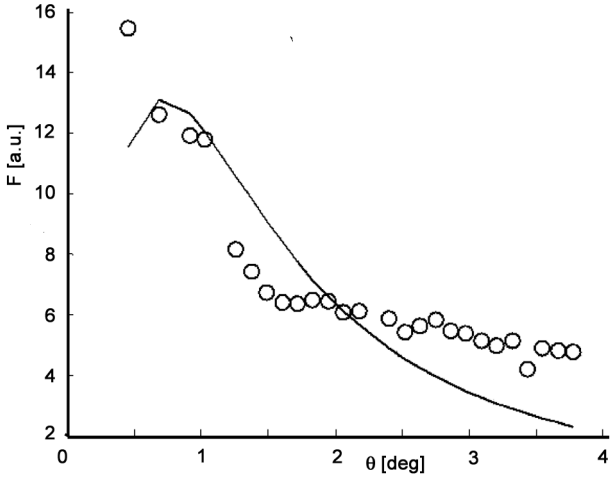

Fig. 5. The plot of the experimental data (circles) and of the calculated *F* function (solid line) for CA sample in function of θ

Considering the significance of the *g* parameter, one can conclude that bigger particles scatter light more isotropic than smaller ones. The size of the scattering centres is smaller than the wavelength and thus the light diffusion may be described by the Rayleigh scattering rather than by the Mie scattering [17, 18]. This might explain the mismatch of the curve to the experimental data. A better match can be found on bigger scattering centers, which can be treated in terms of the Mie scattering, better described by the Henyey Greenstein phase function. In this paper, the experimental results of the light scattering anisotropy have been presented, without any theoretical explanation on the difference in the *g* parameter.

4. Conclusions

Physical characterization of two samples of aqueous suspensions of magnetic nanoparticles stabilized with citric acid (CA) and perchloric acid (PA), synthesized by the same protocols was discussed. The highest viscosity and volume fraction were evidenced for the magnetic nanoparticles coated with citric acid. The high magnetization value and small magnetic diameter of coated nanoparticles were found for the sample based on citric acid coating. The IR spectra confirmed the presence of iron perchlorate in the solid phase of the PA sample and the presence of citric acid at the magnetite surface in the CA samples. The anisotropy parameter *g* of the PA sample was higher than that of the CA sample.

References

[1] PAPEL S.S., US Patent, 3 (1965), 572.
[2] KHALAFALLA S.E., REIMERS G.W., IEEE Trans. Magn., 16 (1980), 178.
[3] ROSENSWEIG R.E., *Ferrohydrodynamics*, Cambridge University Press, New York, 1985.
[4] SCHERER C., FIGUEIREDO NETO A.M., Brazil. J. Phys., 35 (2005), 718.
[5] MENDENHALL G.D., GENG Y., HWANG J., J. Colloid Interface Sci., 184 (1996), 519.
[6] FAUCONNIER N., BÉE A., ROGER J., PONS J.N., J. Molecular Liquids, 83 (1999), 233.
[7] SOUSA M.H., RUBIM J.C., SOBRINHO P.G., TOURINHO F.A., J. Magn. Magn. Mater., 225 (2001), 67.
[8] CORNEANU G.C., CORNEANU M., MARINESCU G., BADEA E., BĂBEANU C., BICA D., COJOCARU L., Abstracts book of 8th Int. Conf. Magn. Fluids, Timisoara, 1998, p. 447.
[9] PAVEL A., TRIFAN M., BARA I.I., CREANGA D.E., COTAE C., J. Magn. Magn. Mater., 201 (1999), 443.
[10] RĂCUCIU M., CREANGĂ D., J. Magn. Magn. Mater., 311 (2007), 288.
[11] RĂCUCIU M., CREANGĂ D., J. Magn. Magn. Mater., 311 (2007), 291.
[12] ENZEL P., ADELMAN N.B., BECKMAN K.J., CAMPBELL D.J., ELLIS A.B., LISENSKY G.C., J. Chem. Educ., 76 (1999), 943.
[13] HAMMER M., SCHWEITZER D., MICHEL B., THAMM E., KOLB A., Appl. Opt., 37 (1998), 7410.
[14] HAMMER M., YAROSLAVSKY A.N., SCHWEITZER D., Phys. Med.Biol., 46 (2001), N65.
[15] STEENBERGEN W., KOLKMAN R., DE MUL F., J. Opt. Soc. Am. A, 16 (1999), 2959.
[16] CHICEA D., RĂCUCIU M., J. Opt. Adv. Mater., 9 (2007), 3843.
[17] GOODMAN J.W., *Series Topics in Applied Physics*, Vol. 9, J.C. Dainty (Ed.), Springer, Berlin, 1984.
[18] BRIERS J.D., Physiol. Meas., 22 (2001), R35.

Received 21 January 2008